Journal of Inorganic Biochemistry 197 (2019) 110700

Contents lists available at ScienceDirect

Journal of Inorganic Biochemistry

journal homepage: www.elsevier.com/locate/jinorgbio

# Inhibition of $Na^+/K^+$- and $Ca^{2+}$-ATPase activities by phosphotetradecavanadate

Gil Fraqueza[a,b,1], Juan Fuentes[b,1], Lukáš Krivosudský[c,d], Saikat Dutta[e], Sib Sankar Mal[e,*], Alexander Roller[f], Gerald Giester[g], Annette Rompel[c,*], Manuel Aureliano[b,h,**]

[a] ISE, University of Algarve, 8005-139 Faro, Portugal
[b] CCMar, University of Algarve, 8005-139 Faro, Portugal
[c] Universität Wien, Fakultät für Chemie, Institut für Biophysikalische Chemie, Althanstr. 14, 1090 Wien, Austria
[d] Comenius University, Faculty of Natural Sciences, Department of Inorganic Chemistry, Mlynská dolina, Ilkovičova 6, 842 15 Bratislava, Slovakia
[e] Department of Chemistry, National Institute of Technology Karnataka, Mangalore 575025, Karnataka, India
[f] Universität Wien, Fakultät für Chemie, Zentrum für Röntgenstrukturanalyse, 1090 Wien, Austria
[g] Universität Wien, Fakultät für Geowissenschaften, Geographie und Astronomie, Institut für Mineralogie und Kristallographie, 1090 Wien, Austria
[h] FCT, University of Algarve, 8005-139 Faro, Portugal

ARTICLE INFO

*Keywords:*
Polyoxometalates
Phosphotetradecavanadate
Decavanadate
P-type ATPases
Epithelial chloride secretion

ABSTRACT

Polyoxometalates (POMs) are promising inorganic inhibitors for P-type ATPases. The experimental models used to study the effects of POMs on these ATPases are usually *in vitro* models using vesicles from several membrane sources. Very recently, some polyoxotungstates, such as the Dawson anion $[P_2W_{18}O_{62}]^{6-}$, were shown to be potent P-type ATPase inhibitors; being active *in vitro* as well as *in ex-vivo*. In the present study we broaden the spectrum of highly active inhibitors of $Na^+/K^+$-ATPase from basal membrane of epithelial skin to the bi-capped Keggin-type anion phosphotetradecavanadate $Cs_{5.6}H_{3.4}PV_{14}O_{42}$ ($PV_{14}$) and we confront the data with activity of other commonly encountered polyoxovanadates, decavanadate ($V_{10}$) and monovanadate ($V_1$). The X-ray crystal structure of $PV_{14}$ was solved and contains two *trans*-bicapped α-Keggin anions $H_xPV_{14}O_{42}^{(9-x)-}$. The anion is built up from the classical Keggin structure $[(PO_4)@(V_{12}O_{36})]$ capped by two [VO] units. $PV_{14}$ (10 μM) exhibited higher *ex-vivo* inhibitory effect on $Na^+/K^+$-ATPase (78%) than was observed at the same concentrations of $V_{10}$ (66%) or $V_1$ (33%). Moreover, $PV_{14}$ is also a potent *in vitro* inhibitor of the $Ca^{2+}$-ATPase activity ($IC_{50}$ 5 μM) exhibiting stronger inhibition than the previously reported activities for $V_{10}$ (15 μM) and $V_1$ (80 μM). Putting it all together, when compared both P-typye ATPases it is suggested that $PV_{14}$ exibited a high potential to act as an *in vivo* inhibitor of the $Na^+/K^+$-ATPase associated with chloride secretion.

## 1. Introduction

Polyoxometalates (POMs) are inorganic anionic metal oxide clusters exhibiting a broad diversity of structures and outstanding properties leading to their application in many fields [1–5]. The usage of biologically active POMs for medical purposes is continuously increasing and thus attracting more and more attention from scientist coming from medical- and biology-related research areas [5–8]. P-type ATPases constitute a large family of ion pumps, which are found in all kingdoms of life and are responsible for many biologically essential processes assigning them important roles in health and diseases [9–12]. Therefore, P-type ATPases represent important pharmacological targets being reflected by the substantial number of drugs targeting these ion pumps [11].

Forty years have passed since the discovery that the muscle inhibitor factor (MIF) and the $Na^+/K^+$-ATPase inhibitor (present in commercial ATP) contained vanadium in the +V oxidation state (as vanadate $VO_4^{3-}$) [13]. Actually, it is well known that vanadate ions or vanadium complexes inhibit or stimulate the activity of many enzymes [14]. In fact, the serendipitous discovery of vanadate as a $Na^+/K^+$-ATPase inhibitor [13] leads us, 40 years after, to the discussion on POMs as putative drugs in the treatment of several diseases in which the molecular targets are established to be precisely the ion pumps such as $Na^+/K^+$-ATPase and $Ca^{2+}$-ATPase [12,14–16]. Furthermore, POMs are

* Corresponding authors.
** Correspondence to: M. Aureliano, CCMar, University of Algarve, 8005-139 Faro, Portugal.
*E-mail addresses:* malss@nitk.edu.in (S.S. Mal), annette.rompel@univie.ac.at (A. Rompel), maalves@ualg.pt (M. Aureliano).
[1] Both authors contributed equally for this manuscript.

https://doi.org/10.1016/j.jinorgbio.2019.110700
Received 15 January 2019; Received in revised form 16 April 2019; Accepted 25 April 2019
Available online 29 April 2019

particularly known as inhibitors of others enzymes such as phosphatases, ecto-ATPases or cholinesterases [6–8,14,17–21]. For the majority of common drugs used in therapy as P-type ATPase inhibitors, the main target is the $Na^+/K^+$-ATPase [11]. These drugs are being investigated for several disease treatments such as heart failure, antipsychotic, antimalaria and also used as anesthetics, tumor promoter, antibiotic and insulin mimetic agents, and, very importantly, they present inhibitory capacity not so different from POMs [11,12]. Previously published data regarding the $Ca^{2+}$-ATPase inhibition are available for decaniobate (abbreviated as $Nb_{10}$) $[Nb_{10}O_{28}]^{6-}$ ($IC_{50}$ = 35 μM) [16] and for Keggin-based polyoxotungstates (POTs) such as mono-substituted Keggin structure $[TiW_{11}CoO_{40}]^{8-}$ (4 μM), tri-lacunary [A-α-$SiW_9O_{34}]^{10-}$ (16 μM) and [B-α-$AsW_9O_{33}]^{9-}$ (20 μM), lacunary Dawson type [α-$H_2P_2W_{12}O_{48}]^{12-}$ (11 μM), and also for $[As_2W_{19}O_{67}(H_2O)]^{14-}$ (28 μM) [22].

Herein, we report and compare for the first time the effects of three polyoxovanadates (POVs), namely phosphotetradecavanadate, $H_xPV_{14}O_{42}^{(9-x)-}$ (abbreviated as $PV_{14}$), monovanadate $H_xVO_4^{(3-x)-}$ ($V_1$) and decavanadate $H_xV_{10}O_{28}^{(6-x)-}$ ($V_{10}$) on the activity of P-type ATPases using two different experimental models: the *in vitro* $Ca^{2+}$-ATPase activity of sarcoplasmic reticulum (SR) vesicles and the *ex-vivo* activity of $Na^+/K^+$-ATPase using a model obtained from basal membrane of epithelial skin. To our knowledge those represent the first *ex-vivo* studies describing the effects of $PV_{14}$ and $V_{10}$ in the processes of epithelial chloride secretion energized by basolateral $Na^+/K^+$-ATPase activity. Furthermore, we also provide full characterization of the $PV_{14}$ prepared as $Cs_{5.6}H_{3.4}PV_{14}O_{42}$ including X-ray crystal structure analysis.

## 2. Experimental section

### 2.1. Materials and characterization methods

Vanadium and cesium contents were determined by ICP-MS using Perkin-Elmer ELAN 6000 instrument. FT-IR spectra were collected on a Bruker Vertex 70 instrument by ATR method. $^{51}V$ nuclear magnetic resonance spectroscopy measurement of 1 mM $PV_{14}$ aqueous solution (with 10% of $D_2O$, 20 °C) was taken on a Bruker AV II + 500 MHz instrument operating at 131.60 MHz for $^{51}V$ nucleus (2500 scans, accumulation time 0.05 s, relaxation delay 0.01 s). Chemical shift values are given with reference to $VOCl_3$ (0 ppm) as a standard.

The X-ray intensity data were measured on a Bruker X8 Apex2 diffractometer equipped with multilayer monochromators, Mo K/α (λ = 0.71073 Å) INCOATEC micro focus sealed tubes and Oxford cooling system. The structure was solved by Patterson methods and refined by full-matrix least-squares techniques. Non-hydrogen atoms were refined with anisotropic displacement parameters. The following software was used: Bruker SAINT software package [23] using a narrow-frame algorithm for frame integration, SADABS [24] for absorption correction, OLEX2 [25] for structure solution, refinement, molecular diagrams and graphical user-interface, Shelxl [26] for refinement and graphical user-interface, SHELXS-2016 [27] for structure solution, SHELXL-2016 [28] for refinement, Platon [29] for symmetry search and check. The graphic for Fig. 1 was obtained with Diamond 4.5.3 [30].

Common analytical solutions, reagents and materials used for the preparation of the calcium pump vesicles and for the kinetic studies described below were prepared from reagents obtained from Sigma-Aldrich (Portugal, Austria). The stock solutions of monovanadate ($V_1$, 50 mM, pH 10.5) and decavanadate ($V_{10}$, 5 mM, pH 4.0) were prepared similarly as in our previous studies on $V_{10}$ interactions with proteins and *in vivo* studies [14,16,17]. Briefly, $NH_4VO_3$ was dissolved in milliQ water with heating, the pH was adjusted to 10.5 with NaOH and the solution was heated until colorless solution was obtained. After cooling, the solution was splitted into two parts. The pH of one of them was adjusted to 4.0 with HCl to obtain an orange solution of $V_{10}$. The other solution is named monomeric vanadate solution $V_1$.

### 2.2. Preparation and characterization of phosphotetradecavanadate

The bicapped Keggin–type phosphotetradecavanadate $Cs_{5.6}H_{3.4}PV_{14}O_{42}{\cdot}12H_2O$ ($PV_{14}$) was synthesized by modification of published procedures [31–33]: $NaVO_3$ (4.5 g, 37 mmol) was dissolved in 40 mL of hot distilled water. $H_3PO_4$ (0.636 mL, 9.3 mmol) was added and the pH was adjusted to 2.5 with conc. $HNO_3$. The solution was heated to 50 °C, CsCl (2 g, 12 mmol) was gradually added into it and the solution was maintained at 50 °C several hours to provide red cubic crystals of the title compound. Elemental analysis for $Cs_{5.6}PV_{14}H_{27.4}O_{54}$ (calc.): V 31.2 (31.3), Cs 29.7 (30.0). Stock solutions (1 mM aqueous solution, pH 5.5) of $PV_{14}$ for inhibition studies were prepared daily wherever adequate by dissolution of the solid compound in water and kept on ice during the utilization.

### 2.3. $Ca^{2+}$-ATPase (in vitro) and $Na^+/K^+$-ATPase (ex-vivo) inhibition studies

Detailed description of experimental procedures necessary for inhibition studies (preparation of sarcoplasmatic reticulum $Ca^{2+}$-ATPase vesicles and epithelial short circuit current in Ussing chambers *ex-vivo*) can be found in [16,22]. In short: Isolated sarcoplasmic reticulum (SR) vesicles prepared from rabbit skeletal muscles as described elsewhere [16] were suspended in 0.1 M KCl, 10 mM HEPES (pH 7.0), diluted 1:1 with 2.0 M sucrose and frozen in liquid nitrogen prior to storage at −80 °C. The ATPase activity and the inhibition of POVs solutions was measured taken into consideration the decrease of the OD (Optical density) per minute in the absence (100% activity) and in the presence of several $PV_{14}$ concentrations, according to described elsewhere [16]. All experiments were performed at least in triplicate. The inhibitory power of the investigated $PV_{14}$ was evaluated determining $IC_{50}$ values meaning the POM concentration inducing 50% of $Ca^{2+}$-ATPase inhibition of the enzyme activity. Aqueous stock solutions of these $PV_{14}$ were prepared in concentrations up to 1 or 0.5 mM stock solution in water considering a $M_r$ of 2380.01 g/mol. Solutions of $PV_{14}$ were prepared daily wherever adequate by dissolution of the solid compounds in water and kept on ice during the utilization to avoid putative POM decomposition.

For the *ex-vivo* study killifish (*F. heteroclitus*, 4–8 g) was collected with fish traps from the saltmarshes of Ria Formosa (Faro) and maintained in Ramalhete Marine Station (CCMar, University of Algarve, Faro, Portugal). All animal protocols were performed under a "Group C" license from the Direcção-Geral de Veterinária, Ministério da Agricultura, do Desenvolvimento Rural e das Pescas, Portugal.

The experimental setup for the *ex-vivo* study is illustrated in Fig. 1A. $ET_{50}$ is the effective time (in minutes) necessary to reach 50% of the maximum effects for each POM concentration. The maximum inhibitory effect (%) of the ATPase activity by the POVs solutions and the effective time ($ET_{50}$) necessary to reach 50% of the maximum effects (in minutes) were measured, taken into consideration the % decrease of short circuit current (Isc, μA/cm$^2$) in the absence (100% activity) and upon addition of $PV_{14}$ (Fig. 1B). In the opercular epithelium of killifish used for our studies, Isc is a direct measure of apical chloride secretion mediated by chloride channels, which relies on an intact basolateral $Na^+/K^+$-ATPase to function [34,35]. Methodology for *ex-vivo* opercular epithelia preparation followed our current methods [22,36]. Fish were anaesthetized with 2-phenoxyethanol (1:2000 *v*/v), sacrificed by decapitation and the cranium was cut longitudinally. The gills and other tissue remains were removed carefully and the epithelial skin covering the opercular bone were dissected out and transferred to fresh-gassed saline (99.7:0.3 $O_2/CO_2$) with the following composition (all values in mM): NaCl, 160; $MgSO_4$, 0.93; $NaH_2PO_4$, 3; $CaCl_2$ 1.5, $NaHCO_3$ 17.85, KCl 3; Glucose 5.5 HEPES 5; pH 7.8. Measurement of short circuit current (Isc, μA/cm$^2$) was performed in symmetric conditions under voltage clamp to 0 mV. Open circuit potential (Vt, mV) and Isc were monitored by means of Ag/AgCl electrodes connected to

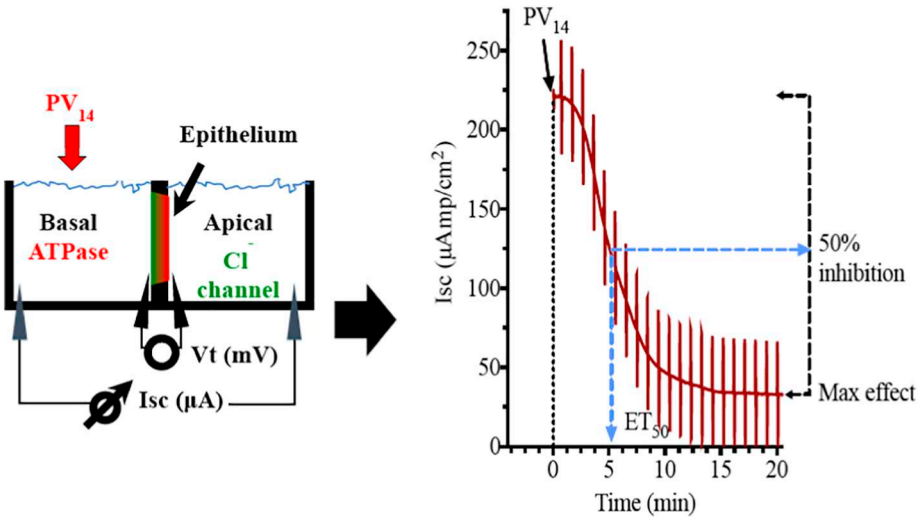


**Fig. 1.** A) Schematic representation of the experimental setup of the opercular epithelium of killifish used for our *ex vivo* studies. Isc was measured in voltage clamp, and in this model represents chloride secretion. The process is energized by basolateral $Na^+/K^+$-ATPase and chloride is secreted apically *via* a chloride channel. B) Original trace of the effect of short circuit current (Isc, μA/cm$^2$) in the opercular epithelium of killifish mounted in Ussing chambers and kept under voltage clamp (Vt = 0 mV) after $PV_{14}$ addition. Effective time 50 ($ET_{50}$), time necessary to reach 50% of the maximum effects is shown in minutes; and maximum inhibitory effects are calculated as the % of basal values.

the chambers by 3 mm bore agar bridges (1 M KCl in 3% agar). Clamping of epithelia to 0 mV and recording of Isc was performed by means of VCC600 voltage clamp amplifiers (Physiologic Instruments, San Diego, USA). Bioelectrical data was continuously digitized trough a Lab-Trax-4 (WPI, Sarasota, US) onto a Macbook laptop using Labscribe3 Software (Iworks systems, Dover, US). All experiments were performed at least in triplicate. Calculations of $ET_{50}$ and Maximum effect were performed using GraphPad Prism version 6.00 for Macintosh (GraphPad Software, La Jolla California USA).

## 3. Results and discussion

### 3.1. Characterization of phosphotetradecavanadate

The non-stochiometric composition found for $Cs_{5.6}H_{3.4}PV_{14}O_{42}{\cdot}12H_2O$ ($PV_{14}$) is in good agreement with the previously reported analogical salts $K_{5.72}H_{3.28}[PV_{14}O_{42}]$ [31] and $Rb_{5.89}H_{3.11}[PV_{14}O_{42}]$ [37]. The characteristic bands in IR spectra represent P—O (1053 *m* $cm^{-1}$) and V═O stretching vibrations (934 *vs* + 862 *s* $cm^{-1}$), as well as vibrations of various V–O–V bridges (two groups of bands at 800, 741, 709 $cm^{-1}$ + 590, 557, 476, 428 $cm^{-1}$) (Fig. S2).

$^{51}V$ NMR spectrum of a 1 mM solution of $PV_{14}$ (Fig. 2) revealed three characteristic peaks at −592 ppm, −574 ppm, −524 ppm in the ratio 4:8:2. The chemical shift at −524 ppm corresponds to vanadium atoms of the two capping V═O units that are pentacoordinated, the remaining peaks corresponds to octacoordinated vanadium atoms of the Keggin cage connected to the capping V atoms through oxido bridges (−574 ppm) or not connected (−592 ppm). Based on published speciation studies in the ternary $H^+/H_2VO_4^-/H_2PO_4^-$ system with found chemical shifts −589 ppm, −572 ppm, −521 ppm for $H_3[PV_{14}O_{42}]^{6-}$ species and −598 ppm, −580 ppm, −530 ppm for $H_4[PV_{14}O_{42}]^{5-}$ species [38], the NMR shows that the found chemical shifts lie in the expected region.

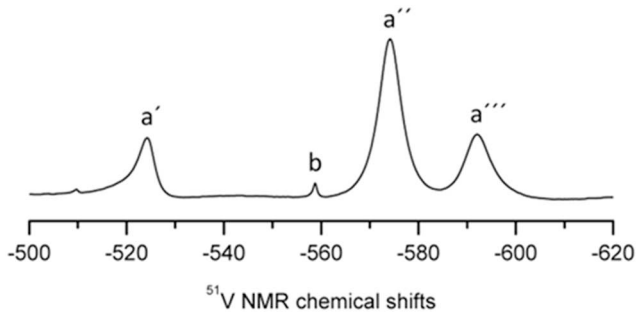


**Fig. 2.** $^{51}V$ NMR spectrum of 1 mM aqueous $PV_{14}$ solution at autogenous pH (5.5). Legend: a′, a″, a‴ $H_xPV_{14}O_{42}^{(9-x)-}$; b $H_3VPO_7^-$.

The X-ray crystal structure of $PV_{14}$ (Fig. S1; Table S2 and Table S3) was solved in *P-4n2* space group and the unit cell contains two *trans*-bicapped α-Keggin anions $H_xPV_{14}O_{42}^{(9-x)-}$ (Fig. 3). The anion is built up from the classical Keggin structure $[(PO_4)@(V_{12}O_{36})]$ capped by two [VO] units. The V═O groups are located in surface moieties formed by four adjacent oxygen atoms at V—O distances in the range 1.838–2.238 Å (Fig. S1). The two [VO] units are in opposition and occupy three different pairs of positions on the surface of the Keggin anion with various occupancies giving the overall sum formula as determined by ICP-MS analysis. The high degree of disorder in the area of counter ions and water molecules forced the use of squeeze. According to the result of elemental analysis (5.6 Cs), the excluded volume (1208.2 Å$^3$) and number of electrons (1112.0), the following maximum content is possible: 12 Cs and up to ~45 $H_2O$ molecules. This leads to ~1112 electrons and ~1200 Å$^3$ by the model. This is in very good accordance to approximately twelve charges of the two POMs in the unit cell needed. The analogous compounds $K_{5.72}H_{3.28}[PV_{14}O_{42}]$ [32] and $Rb_{5.89}H_{3.11}[PV_{14}O_{42}]$ [37] also exhibited the same disorder that was treated similarly.

### 3.2. Inhibition of $Ca^{2+}$-ATPase by phosphotetradecavanadate: in vitro studies

The effect of phosphotetradecavanadate ($PV_{14}$) on the activity of sarcoplasmic reticulum $Ca^{2+}$-ATPase from skeletal muscle (*in vitro*

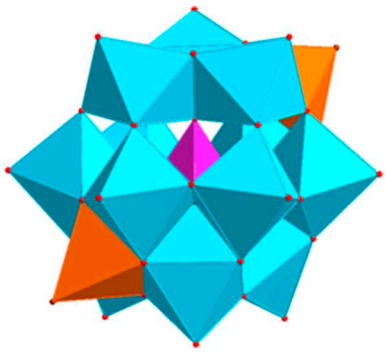

**Fig. 3.** Polyhedral representation of the structure of $H_xPV_{14}O_{42}^{(9-x)-}$ anion in $PV_{14}$ as revealed by X-ray structure analysis. Polyhedron legend: pink {$PO_4$}, blue {$VO_6$}, orange {VO} capping unit.

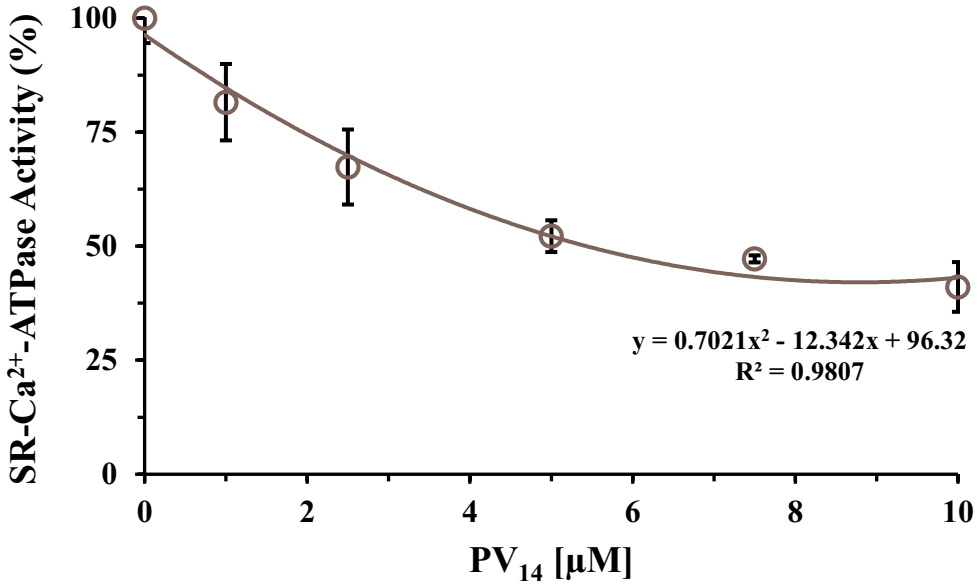


**Fig. 4.** Inhibition of $Ca^{2+}$-ATPase activity by $PV_{14}$. $Ca^{2+}$-ATPase was measured spectrophotometrically at 340 nm and 22 °C, using the coupled enzyme pyruvate kinase/lactate dehydrogenase assay. The experiments were initiated after the addition of 10 µg/mL calcium ATPase, in the presence or absence of 4% (*w*/w) of calcium ionophore A23187. Data are plotted as means ± SD. The results shown are the average of triplicate experiments.

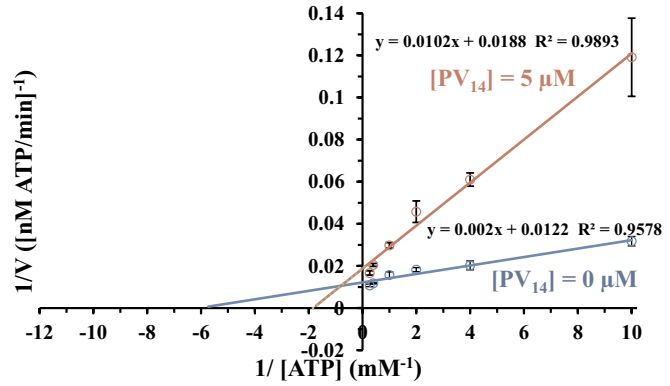


**Fig. 5.** Lineweaver-Burk plots of $Ca^{2+}$-ATPase activity in the absence (blue) and in the presence (orange) of 5 µM of the polyoxometalate $PV_{14}$.The plots were used for determining the type of enzyme inhibition. The POM $PV_{14}$ presented a mixed type of inhibition. Data are plotted as means ± SD. The results shown are the average of triplicate experiments.

model) was investigated. It was observed that $PV_{14}$ inhibits the $Ca^{2+}$-ATPase activity, expressed as a percentage of the control obtained without inhibitor, in a concentration dependent manner (Fig. 4). The inhibitory power of $PV_{14}$ was evaluated using $IC_{50}$ values (POM concentration at which it induces 50% of $Ca^{2+}$-ATPase inhibition of the enzyme activity) and the $IC_{50}$ value of 5.4 ± 0.5 µM was obtained. $Ca^{2+}$-ATPase $IC_{50}$ values of inhibition below 1 µM were previously determined for polyoxotungstates (POTs) such as $[\alpha\text{-}P_2W_{18}O_{62}]^{6-}$ (0.6 µM) and $[H_{10}Se_2W_{29}O_{103}]^{14-}$ (0.3 µM), whereas the lowest potency was observed for $[TeW_6O_{24}]^{6-}$ ($IC_{50}$ = 200 µM) [22]. It was previously determined that decavanadate $V_{10}$ ($IC_{50}$ = 15 µM) is more potent $Ca^{2+}$-ATPase inhibitors than $V_1$ ($IC_{50}$ = 80 µM). Herein, we show that $PV_{14}$ is the strongest inhibitor of the calcium pump ($IC_{50}$ = 5 µM) among so far investigated vanadates. For both $Nb_{10}$ and $V_{10}$, it was previously observed that they showed to be $Ca^{2+}$-ATPase non-competitive inhibitors regarding the natural ligand Mg-ATP [16]. $PV_{14}$ presented a mixed type inhibition (Fig. 5), as was previously observed for $[\alpha\text{-}P_2W_{18}O_{62}]^{6-}$ and $[TeW_6O_{24}]^{6-}$ [22] suggesting that it can interact with the $Ca^{2+}$-ATPase whether or not the enzyme has already bound substrate and pointing out to the existence of two distinct protein binding sites for these types of POMs. Only for $V_{10}$ a binding site in the $Ca^{2+}$-ATPase was previously described, involving at least three protein domains including the phosphorylation and the nucleotide binding sites [39]. Studies about the type of inhibition and the mechanism of action of the other POMs interactions with P-type ATPases are to our knowledge still to be determined [16,17,22].

### 3.3. Inhibition of $Na^+/K^+$-ATPase by phosphotetradecavanadate: ex-vivo studies

As pointed out in Fig. 1, modification of Isc provides an immediate read-out of inhibitory/stimulatory effects on either the apical chloride channel, or the basolateral $Na^+/K^+$-ATPase induced by $PV_{14}$. Isc is measured in voltage clamp, and in this model represents chloride secretion. The process is energized by basolateral $Na^+/K^+$-ATPase and chloride is secreted apically *via* a chloride channel. In this polarized epithelium, both mechanisms are required to be intact to sustain the process of secretion. Therefore, inhibitory effects of POMs on the basolateral side (where $Na^+/K^+$-ATPase is located) result in inhibitory effects on Isc. Herein, it was observed that when $PV_{14}$ was added to the basal side (Fig. 1), it does inhibit the $Na^+/K^+$-ATPase activity (expressed as the % of maximum inhibition, in a concentration dependent manner, Fig. 6A). Thus, for 10 µM a maximum inhibition of 78% of the basal current was observed whereas a 50% inhibition is obtained for even less than 1 µM $PV_{14}$. On the other hand, the addition of $PV_{14}$ to the apical side was not accompanied by an effect on Isc, ruling out chloride channels as putative targets of $PV_{14}$, at least in a range of concentrations up to 10 µM. From the data of Fig. 6A, we calculated an $IC_{50}$ values of 1.4 ± 0.1 µM for the *ex-vivo* $Na^+/K^+$-ATPase inhibition. In addition, it has to be noted that besides the maximum inhibitory effect (providing information about inhibitor efficacy) also $ET_{50}$ values (providing information about inhibition velocity) can be appreciated to characterize the biological effects of the inhibitor. It was observed that the value of $ET_{50}$ decreases from 21 to 7 min upon increasing $PV_{14}$ concentration (Fig. 6B). When comparing different POMs, this negative correlation does necessary mean that the lowest $ET_{50}$ value implies a higher inhibition. In fact, it was observed that decavanadate at the same concentration (10 µM) exhibits the maximum inhibition of 66% and an $ET_{50}$ of 14 min; whereas for the monomeric vanadate (at 10 µM) only 33% of maximum inhibition was observed, but a lower $ET_{50}$ was determined (6 min).

A simultaneous comparison of these three vanadate species, $PV_{14}$, $V_{10}$ and $V_1$ at the same concentration of 10 µM (Fig. 7) clearly illustrates that $PV_{14}$ (blue line) is the most potent *ex-vivo* inhibitor (78%

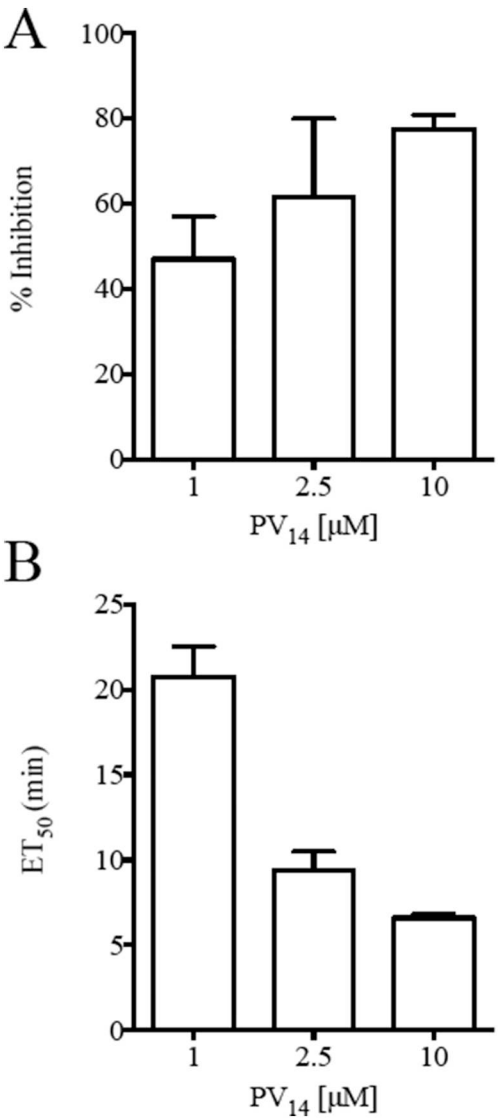


**Fig. 6.** A) Maximum inhibitory effects are calculated as the % of basal values and B) Effective time 50 ($ET_{50}$), time necessary to reach 50% of the maximum effects (shown in minutes); obtained for 1, 2.5 and 10 μM $PV_{14}$ concentrations. Data are plotted as means ± SD. The results shown are the average of triplicate experiments at 22 °C.

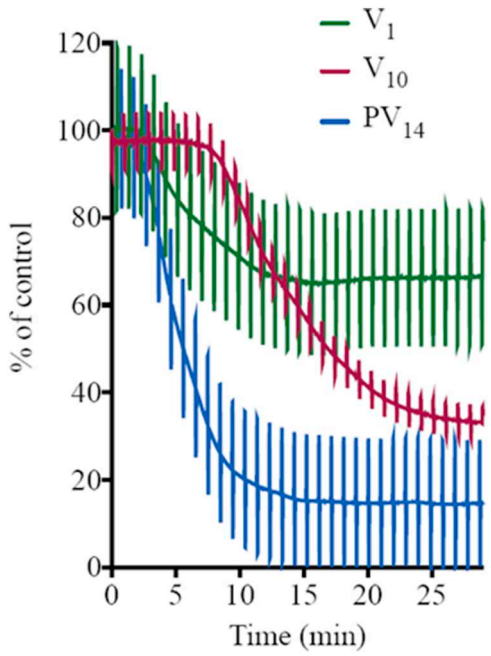


**Fig. 7.** $PV_{14}$, $V_{10}$ and $V_1$ inhibition (%) of the $Na^+/K^+$-ATPase activity from basal membrane of the skin epithelia. $PV_{14}$ (10 μM) inhibited 78% with an $ET_{50}$ of 6.4 min (blue) whereas lower effects were observed for $V_{10}$ (red) (66% inhibition, $ET_{50}$ 13.7) and for $V_1$ (green) (33% and $ET_{50}$ 6.4 min). Perpendicular lines were used to calculate tissue resistance. As it can be observed, the *ex vivo* epithelia preparations retained integrity and selectivity after compounds exposure.

after 30 min upon addition), whereas for decavanadate (red) and vanadate (green) only minor effects were observed. It can be also observed, a constant height of the current deflections used to calculate tissue resistance implying that the *ex-vivo* preparation maintained its integrity and selectivity before and after POM exposure (Fig. 7). For these studies a positive control experiment was performed with the conventional $Na^+/K^+$-ATPase inhibitor ouabain. Ouabain (at 10 μM) showed a maximum inhibition value of 100% and an $ET_{50}$ of 3.2 min [22]. By inhibiting the basolateral $Na^+/K^+$-ATPase activity, ouabain concomitantly prevents apical chloride secretion. $Cs^+$, in contrast with rubidium, is known not to affect the activity of this type of enzyme [40].

Let us briefly comment on the mechanism of P-type ATPases inhibition by POMs. POMs clearly exhibit different types of interaction with different P-type ATPases [12,14]. For example, the orthotungstate ($HWO_4^{2-}$) presents a very low inhibition capacity ($IC_{50}$ = 1.5 mM) for the $Na^+/K^+$-ATPase [15], while for another ion pump, SR $Ca^{2+}$-ATPase is the $IC_{50}$ = 400 μM [16]. Herein, taking into account the $Ca^{2+}$-ATPase $IC_{50}$ values of inhibition for $PV_{14}$ ($IC_{50}$ = 5 μM) and $V_{10}$ ($IC_{50}$ = 15 μM) apparently the lower negative charge (−6) for $V_{10,}$ at physiological pH and according to its pKas values [14,16], in comparison to $PV_{14}$ (−9) is not favoring enzyme inhibition. Very recently, for high affinity POTs, exhibiting $IC_{50}$ values lower than 16 μM, it was described a correlation between their activity ($IC_{50}$ value) and their charge density, as well as by volume of POM anion [22]. Also recently, a combination of NMR studies, *ab initio* calculations and crystallographic analysis point out to specific molecular interactions between $H_3PW_{12}O_{40}$ or $H_4SiW_{12}O_{40}$ and the $Na^+/K^+$-ATPase [41]. POMs-protein interactions observed previously with myosin, actin and calcium ATPase [12,14,16,17,22,42,43] were described to be mostly of electrostatic nature including hydrogen bonds, but could also involve direct interaction with cysteins, as described for the P-type ATPase and actin [17,43]. Thus, besides electrostatic interactions, specific bonding modes underpinning their relative affinities and site recognition, and the structure and accessibility of the ATPase site for each crystallographically defined enzyme/pump relative to the inhibitory effectiveness of each POM are still to be determined [44–46]. In conclusion, the study of protein-POMs interactions is of utmost importance to explain and improve inhibition of certain enzymes for potential drug development [47–49].

As referred above, only few studies described POMs as inhibitors of the hydrolytic activity of several P-type ATPases [15,16]. In these P-type ATPases studies, normally vesicles from cellular membranes or organelles are used and constitute *in vitro* models for the study of POMs toxicity effects. However, in the majority of these studies, the stability, as well others factors, of the compounds and/or the putative decomposition into others species are not taken in consideration. Thus, this possibility must be considered and several papers were published over the last years [49–56]. Therefore, if the polyoxometalates species responsible for the observed effects are not always possible to be determined, participation of other species than the ones initially added to the biological system should be taken into account [49–57].

In fact, regarding the *in vitro* studies of POMs for the P-type ATPases

[15,16] it is possible to find, for instance, different experimental conditions such as temperature (25 and 37 °C), different times upon incubation depending on the kinetic studies used (2, 15 or 30 min) and of course different concentration range due to different $IC_{50}$ values of ATPase activity inhibition. After incubation, both higher temperature and time would favor the decomposition of the added POM and therefore the appearance of different species that might also have a contribution for the observed inhibitory effects.

In this paper, the temperature was maintained for both *in vitro* and *ex-vivo* studies but the time after addition of the $PV_{14}$ were clearly different, 1 min for the $Ca^{2+}$-ATPase assays, and 5 to 10 min incubation for the $Na^+/K^+$-ATPase assays. The determination of the inhibitory capacity needs also different times, 2–3 min for the $Ca^{2+}$-ATPase and 30 min for the $Na^+/K^+$-ATPase. Moreover, the mediums are different and also with slight different pH values. Therefore, the experimental conditions are not always favoring the putative comparison with different experimental conditions and methodologies.

In previous studies with $V_{10}$ and $Ca^{2+}$-ATPase and other muscle proteins (such as myosin and actin) the putative reduction of vanadate was always taken in consideration [14,43,49]. In fact, reduction of $V_{10}$ to oxidovanadium(IV) ($VO^{2+}$), was previously observed upon actin interaction, but only after 90 min incubation and with huge amounts of protein. Moreover, in the presence of the natural ligand (ATP) the vanadate reduction was not observed, suggesting that decavanadate interaction at the actin ATP binding is needed for the reduction of vanadate [43,49]. Herein, at the experimental *in vitro* and *in vivo* conditions the redox stability of $PV_{14}$ during the biological measurements would be hard or impossible to be determined not only because of the concentrations used, in the order of microM, but also because of the time upon exposition, that is in the scale of a few minutes. Still, it is well known that intracellular V(V) can be reduced to oxidovanadium (IV) [58–61].

Putting it all together, and taking into account the $IC_{50}$ values determined, the Keggin type polyoxovanadate $PV_{14}$ exibited a high potential to act as an *in vivo* inhibitor of the $Na^+/K^+$-ATPase than $V_{10}$ or $V_1$. However, as referred before for $V_{10}$ [49], and also due to the vanadium complex chemistry and biochemistry we cannot exclude that besides $PV_{14}$ the observed effects might be due to other vanadate or even to vanadyl species. Therefore, strong efforts are needed to confirm the biologically active POMs species.

## 4. Conclusions

The X-ray crystal structure of $PV_{14}$ was solved and contains two *trans*-bicapped α-Keggin anions $H_xPV_{14}O_{42}{}^{(9-x)-}$. The anion is built up from the classical Keggin structure $[(PO_4)@(V_{12}O_{36})]$ capped by two [VO] units. Phosphotetradecavanadate ($Cs_{5.6}H_{3.4}PV_{14}O_{42}{\cdot}12H_2O$) synthesized and characterized in this work is the best so far investigated member of the alkali metals family of phosphotetradecavanadates, therefore it was reasonable to employ it in the inhibition studies of P-type ATPases. $Ca^{2+}$-ATPase activity from sarcoplasmic reticulum is inhibited by $PV_{14}$ with the $IC_{50} = 5\,\mu M$. This is about ten times higher than $IC_{50}$ values reported for highly active POMs such as $[\alpha\text{-}P_2W_{18}O_{62}]^{6-}$ (0.6 μM), but on the other hand $PV_{14}$ is 3 times more potent than $V_{10}$ (15 μM) and much more potent than $Nb_{10}$ (35 μM) and $[TeW_6O_{24}]^{6-}$ (≈200 μM). Similarly as described before for $[\alpha\text{-}P_2W_{18}O_{62}]^{6-}$ and $[TeW_6O_{24}]^{6-}$ a mixed type of inhibition was observed for $PV_{14}$. Therefore, a different mode of interaction with the $Ca^{2+}$-ATPase than the one observed for $V_{10}$ and $Nb_{10}$ (shown to be non-competitive inhibitors) must be involved. However, $PV_{14}$ was shown to be the most potent $Na^+/K^+$-ATPase inhibitor when using an *ex-vivo* model obtained from basal membrane of the skin epithelia. Thus, for the *ex-vivo* $Na^+/K^+$-ATPase activity an $IC_{50}$ value of 1.4 μM was observed. This *ex-vivo* model seems to be a very specific model to study the effects of POMs in the processes of epithelial chloride secretion energized by basolateral $Na^+/K^+$-ATPase activity.

## Abbreviations

| | |
|---|---|
| $IC_{50}$ | concentration that induces 50% of $Ca^{2+}$-ATPase inhibition of the enzyme activity |
| $ET_{50}$ | the effective time (in minutes) necessary to reach 50% of the maximum effects. |
| $Nb_{10}$ | decaniobate, niobate oligomer containing 10 niobate units |
| POMs | Polyoxometalates |
| POTs | Polyoxotunsgtates |
| POVs | Polyoxovanadates |
| $PV_{14}$ | phosphotetradecavanadate |
| SR | sarcoplasmic reticulum |
| $V_1$ | vanadate, monomeric vanadate containing 1 vanadate units |
| $V_{10}$ | decavanadate, vanadate oligomer containing 10 vanadate units |

## Acknowledgments

MA thanks to national funds through FCT, Foundation for Science and Technology (UID/Multi/04326/2013; SFRH/BSAB/129821/2017). This research was funded by the Austrian Science Fund (FWF): P27534 (AR) and M2200 (LK). SSM thanks to Council of Scientific & Industrial Research (CSIR) for providing financial support (01(2906)/17/EMR-II). This work was supported by the Grant Agency of the Ministry of Education of the Slovak Republic and Slovak Academy of Sciences VEGA Project No. 1/0507/17. The authors are grateful to Professor Markus Galanski (Universität Wien, Wien) for NMR measurements and Dr. Marek Bujdoš (Comenius University, Bratislava) for ICP-MS analysis.

## Appendix A. Supplementary data

Supplementary data CCDC 1886317 contains the supplementary crystallographic data for $PV_{14}$. These data can be obtained free of charge *via* http://www.ccdc.cam.ac.uk/conts/retrieving.html, or from the Cambridge Crystallographic Data Centre, 12 Union Road, Cambridge CB2 1EZ, UK; fax: +44 1223 336 033; or e-mail: deposit@ccdc.cam.ac.uk. These data include experimental details on inhibition studies, crystal data and structure refinement details. MOL files and InChiKeys of the most important compounds described in this article. Supplementary data to this article can be found online at doi:https://doi.org/10.1016/j.jinorgbio.2019.110700.

## References

[1] X. Chen, S. Yan, H. Wang, Z. Hu, X. Wang, M. Huo, Carbohydr. Polym. 117 (2015) 673–680.
[2] S.S. Wang, G.Y. Yang, Chem. Rev. 115 (2015) 4893–4962.
[3] L. Mohapatra, K.M. Parida, Phys. Chem. Chem. Phys. 16 (2014) 16985–16996.
[4] M.A. Moussawi, N. Leclerc-Laronze, S. Floquet, P.A. Abramov, M.N. Sokolov, S. Cordier, A. Ponchel, E. Monflier, H. Bricout, D. Landy, M. Haouas, J. Marrot, E. Cadot, J. Am. Chem. Soc. 139 (2017) 12793–12803.
[5] A. Bijelic, A. Rompel, Acc. Chem. Res. 50 (2017) 1441–1448.
[6] T. Sun, W. Cui, M. Yan, G. Qin, W. Guo, H. Gu, S. Liu, Q. Wu, Adv. Mater. 28 (2016) 7397–7404.
[7] A. Galani, V. Tsitsias, D. Stellas, V. Psycharis, C.P. Raptopoulou, A. Karaliota, J. Inorg. Biochem. 142 (2015) 109–117.
[8] S. Treviño, D. Velázquez-Vázquez, E. Sánchez-Lara, A. Diaz-Fonseca, J.A. Flores-Hernandez, A. Pérez-Benítez, E. Brambila-Colombres, E. González-Vergara, Oxidative Med. Cell. Longev. 2016 (2016) 605870514 pages.
[9] P.L. Pedersen, E. Carafoli, Trends Biochem. Sci. 12 (1987) 146–150.
[10] C. Toyoshima, M. Nakasako, H. Nomura, H. Ogawa, Nature 405 (2000) 647–655.
[11] L. Yatime, M.J. Buch-Pedersen, M. Musgaard, J.P. Morth, A.-M.L. Winther, B.P. Pedersen, C. Olesen, J.P. Andersen, B. Vilsen, B. Schiøtt, M.G. Palmgre, J.V. Møller, P. Nissen, N. Fedosova, Biochim. Biophys. Acta 1787 (2009) 207–220.
[12] M. Aureliano, G. Fraqueza, C.A. Ohlin, Dalton Trans. 42 (2013) 11770–11777.
[13] L.C. Cantley Jr., L. Josephson, R. Warner, M. Yanagisawa, C. Lechene, G. Guidotti, J. Biol. Chem. 252 (1977) 7421–7423.
[14] M. Aureliano, D.C. Crans, J. Inorg. Biochem. 103 (2009) 536–546.
[15] M.B. Čolović, D.V. Bajuk-Bogdanović, N.S. Avramović, I.D. Holclajtner-Antunović, N.S. Bošnjaković-Pavlović, V.M. Vasić, D.Z. Krstić, Bioorg. Med. Chem. 19 (2011) 7063–7069.

[16] G. Fraqueza, C.A. Ohlin, W.H. Casey, M. Aureliano, J. Inorg. Biochem. 107 (2012) 82–89.
[17] G. Fraqueza, L.A.E. Batista de Carvalho, M. Paula, M. Marques, L. Maia, C. André Ohlin, W.H. Casey, M. Aureliano, Dalton Trans. 41 (2012) 12749–12758.
[18] H. Stephan, M. Kubeil, F. Emmerling, C.E. Müller, Eur. J. Inorg. Chem. 10–11 (2013) 1585–1594.
[19] S.H. Saeed, R. Al-Oweini, A. Haider, U. Kortz, J. Iqbal, Toxicol. Rep. 1 (2014) 341–352.
[20] S.Y. Lee, A. Fiene, W. Li, T. Hanck, K.A. Brylev, V.E. Fedorov, J. Lecka, A. Haider, H.J. Pietzsch, H. Zimmermann, J. Sévigny, U. Kortz, H. Stephan, C.E. Müller, Biochem. Pharmacol. 93 (2015) 171–181.
[21] J. Iqbal, M. Barsukova-Stuckart, M. Ibrahim, S.U. Ali, A.A. Khan, U. Kortz, Med. Chem. Res. 22 (2013) 1224–1228.
[22] N.I. Gumerova, L. Krivosudský, G. Fraqueza, J. Breibeck, E. Al-Sayed, E. Tanuhadi, A. Bijelic, J. Fuentes, M. Aureliano, A. Rompel, Metallomics 10 (2018) 287–295.
[23] Bruker SAINT v8.37A & V7.68A Copyright © 2005–2018 Bruker AXS.
[24] G.M. Sheldrick, SADABS, University of Göttingen, Germany, 1996.
[25] O.V. Dolomanov, L.J. Bourhis, R.J. Gildea, J.A.K. Howard, H. Puschmann, J.: OLEX2: a complete structure solution, refinement and analysis program, J. Appl. Crystallogr. 42 (2009) 339–341.
[26] C.B. Huebschle, G.M. Sheldrick, B. Dittrich, ShelXle: a Qt graphical user interface for SHELXL, J. Appl. Crystallogr. 44 (2011) 1281–1284.
[27] G.M. Sheldrick, SHELXS v 2016/4, University of Göttingen, Germany, 2015.
[28] G.M. Sheldrick, SHELXL v 2016/4, University of Göttingen, Germany, 2015.
[29] A.L. Spek, Structure validation in chemical crystallography, Acta Cryst D65 (2009) 148–155.
[30] Diamond - Crystal and Molecular Structure Visualization. Crystal Impact - Dr. H. Putz & Dr. K. Brandenburg GbR, Kreuzherrenstr. 102, 53227 Bonn, Germany. http://www.crystalimpact.com/diamond
[31] R. Kato, A. Kobayashi, Y. Sasaki, Inorg. Chem. 21 (1982) 240–246.
[32] K. Nomiya, K. Kato, M. Miwa, Polyhedron 5 (1986) 811–813.
[33] S. Uematsu, Z. Quan, Y. Suganuma, N. Sonoyama, J. Power Sources 217 (2012) 13–20.
[34] K.J. Karnaky Jr., K.J. Degnan, J.A. Zadunaisky, Science 195 (1977) 203–205.
[35] J.A. Zadunaisky, The chloride cell: the active transport of chloride and the paracellular pathways, in: W.S. Hoar, D.J. Randall (Eds.), Fish Physiology, XB, Academic Press, New York, 1984, pp. 129–176.
[36] J.A. Martos-Sitcha, G. Martínez-Rodríguez, J.M. Mancera, J. Fuentes, Comp. Biochem. Physiol. A Physiol. 182 (2015) 93–101.
[37] E.V. Murashova, A.B. Iluikhin, N.N. Chudinova, Russ. J. Inorg. Chem. 46 (2001) 1292–1295.
[38] I. Andersson, A. Gorzsás, C. Kerezsi, I. Tóth, L. Pettersson, Dalton Trans. (2005) 3658–3666.
[39] S. Hua, G. Inesi, C. Toyoshima, J. Biol. Chem. 275 (2000) 30546–30550.
[40] R. Krulík, I. Farská, J. Prokeš, Neuropsychobiology 3 (1977) 129–134.
[41] N. Bošnjaković-Pavlović, D. Bajuk-Bogdanović, J. Zakrzewska, Z. Yan, I. Holclajtner-Antunović, J.-M. Gillet, A. Spasojević-de Biré, J. Inorg. Biochem. 176 (2017) 90–99.
[42] T. Tiago, P. Martel, C. Gutiérrez-Merino, M. Aureliano, Biochim. Biophys. Acta 1774 (2007) 474–480.
[43] M.P.M. Marques, D. Gianolio, S. Ramos, L.A.E. Batista de Carvalho, M. Aureliano, Inorg. Chem. 56 (2017) 10893–10903.
[44] A. Bijelic, A. Rompel, Coord. Chem. Rev. 299 (2015) 22–38.
[45] A. Solé-Daura, V. Goovaerts, K. Stroobants, G. Absillis, P. Jiménez-Lozano, J.M. Poblet, J.D. Hirst, T.N. Parac-Vogt, J.J. Carbó, Chem. Eur. J. 22 (2016) 15280–15289.
[46] M. Arefian, M. Mirzaei, H. Eshtiagh-Hosseini, A. Frontera, Dalton Trans. 46 (2017) 6812–6829.
[47] A. Bijelic, M. Aureliano, A. Rompel, Chem. Commun. 54 (2018) 1153–1169.
[48] A. Bijelic, M. Aureliano, A. Rompel, Angew. Chem. Int. Ed. 58 (2019) 2980–2999.
[49] M. Aureliano, Oxidative Med. Cell. Longev. 2016 (2016) 61034578 pages.
[50] A. Levina, D.C. Crans, P.A. Lay, Coord. Chem. Rev. 352 (2017) 473–498.
[51] A. Levina, P.A. Lay, Chem. Asian J. 12 (2017) 1692–1699.
[52] M. Le, O. Rathje, A. Levina, P.A. Lay, J. Biol. Inorg. Chem. 22 (2017) 663–672.
[53] K.A. Doucette, K.N. Hassell, D.C. Crans, K.A. Doucette, J. Inorg. Biochem. 165 (2016) 56–70.
[54] T. Jakusch, T. Kiss, Coord. Chem. Rev. 351 (2017) 118–126.
[55] D. Sanna, V. Ugone, G. Micera, P. Bugly,ó, L. Bír,ó, E. Garribba, Dalton Trans. 46 (2017) 8950–8967.
[56] D. Sanna, J. Palomba, G. Lubinu, P. Buglyó, S. Nagy, F. Perdih, J. Med. Chem. 62 (2019) 654–664.
[57] R. Prudent, V. Moucadel, B. Laudet, C. Barette, L. Lafanechère, B. Hasenknopf, J. Li, S. Bareyt, E. Lacôte, S. Thorimbert, M. Malacria, P. Gouzerh, C. Cochet, Chem. Biol. 15 (2008) 683–692.
[58] M. Garner, J. Reglinski, W.E.J. Mcmurray, I. Abdullah, R. Wilson, J. Biol. Inorg. Chem. 2 (1997) 235–241.
[59] T. C. Delgado, A. I. Tomaz, I. Correia, J. C. Pessoa, J.G. Jones, C.F. Geraldes et al., J. Inorg. Biochem. 99 (2005) 2328–2339.
[60] T. Jakusch, É.A. Enyedy, K. Kozma, Z. Paár, A. Bényei, T. Kiss, Inorg. Chim. Acta 420 (2014) 92–102.
[61] D. Sanna, M. Serra, G. Micera, E. Garribba, Inorg. Chem. 53 (2014) 1449–1464.